Optimal Periodic Control of a Continuous "Living" Anionic Polymerization. III. Presence of Impurities in the Monomer Feed

J. R. VEGA, G. L. FRONTINI,* and G. R. MEIRA†

INTEC, CONICET and Universidad Nacional del Litoral, C.C. 91, (3000) Santa Fe, Argentina

SYNOPSIS

Previous publications have demonstrated that when "living" anionic polymerizations are carried out in continuous reactors under forced periodic operation of the feed flows then: (a) In the absence of impurities and within certain limitations, it is possible to produce polymers with any prespecified values of the number-average chain length, the polydispersity and the polymer production; and (b) even small concentrations of impurities in the monomer feed, drastically inhibit such a possibility. In this work, the optimal periodic control problem has been reformulated, including the presence of impurities. In all cases, the flexibility of the control is reduced with respect to the impurities-free case.

INTRODUCTION

Consider a "living" anionic homopolymerization carried out in a continuous stirred-tank reactor (CSTR), and operated in the steady state (SS). When a deactivating impurity is introduced with the monomer feed, and for all other parameters constant, the produced polymer exhibits the following characterstics[1]: (a) the number-average chain length μ_n and the weight-average chain length μ_w decrease monotonically as the impurities concentration is increased; and (b) under ideal conditions, a Schulz–Flory MWD (with a fixed polydispersity $D_n = \mu_w/\mu_n \cong 2$) is observed.

In Part II of the series,[2] it was theoretically shown that (within certain limitations) polymers with any prespecified average values of μ_n, D_n, and the polymer production z could be produced through periodic oscillations of the initiator and the monomer solutions feed flows. However, in Alassia et al.[1], it was demonstrated that such flexibility could be dramatically reduced by even small quantities of impurities in the monomer feed. In this work, the optimal periodic control problem is reformulated, for a more complex system model that includes impurities.

PROBLEM STATEMENT

The System

Consider an anionic homopolymerization carried out in an isothermal and ideally stirred reactor, with the following reaction mechanism:

$$\mathrm{I} + \mathrm{M} \xrightarrow{k_i} \mathrm{N}_1 \qquad \text{(initiation)} \qquad (1a)$$

$$\mathrm{N}_j + \mathrm{M} \xrightarrow{k_p} \mathrm{N}_{j+1} \quad (j = 1, 2, \cdots) \qquad \text{(propagation)} \qquad (1b)$$

$$\mathrm{N}_j + \mathrm{K} \xrightarrow{k_{t_1}} \mathrm{P}_j \quad (j = 1, 2, \cdots) \qquad \text{(termination)} \qquad (1c)$$

$$\mathrm{I} + \mathrm{K} \xrightarrow{k_{t_2}} \mathrm{IK} \qquad \text{(initator deactivation)} \qquad (1d)$$

where I, M, N_j, K, P_j, and IK, respectively, represent the initiator, the monomer, the "living" polymer of chain length j, the impurity, the deactivated polymer, and the deactivated initiator.

Assume the previous mechanism to be carried out

* Present address: INTEMA (CONICET and Universidad Nacional de Mar del Plata), (7600) Mar del Plata, Argentina.
† To whom correspondence should be addressed.

Journal of Applied Polymer Science, Vol. 42, 3181–3193 (1991)
 CCC 0021-8995/91/123181-13$04.00

in an homogeneous CSTR, and that the monomer and all polymer species have the same density. Then, from the basic mass balances presented in Alassia et al.,[1] the following state model may be derived:

$$\frac{d[I(t)]}{dt} = \frac{1}{V} f_I(t)[I^f] - \frac{f_I(t) + f_M(t)}{V}[I(t)] - k_i[I(t)][M(t)] - k_{t_2}[I(t)][K(t)] \quad (2a)$$

$$\frac{d[M(t)]}{dt} = \frac{1}{V} f_M(t)[M^f] - \frac{f_I(t) + f_M(t)}{V}[M(t)] - k_i[I(t)][M(t)] - k_p[M(t)]\lambda_0(t) \quad (2b)$$

$$\frac{d[K(t)]}{dt} = \frac{1}{V} f_M(t)[K^f] - \frac{f_I(t) + f_M(t)}{V}[K(t)] - k_{t_2}[I(t)][K(t)] - k_{t_1}[K(t)]\lambda_0(t) \quad (2c)$$

$$\frac{d\lambda_0(t)}{dt} = k_i[I(t)][M(t)] - \frac{f_I(t) + f_M(t)}{V}\lambda_0(t) - k_{t_1}[K(t)]\lambda_0(t) \quad (2d)$$

$$\frac{d\lambda_1(t)}{dt} = k_i[I(t)][M(t)] - \frac{f_I(t) + f_M(t)}{V}\lambda_1(t) + k_p[M(t)]\lambda_0(t) - k_{t_1}[K(t)]\lambda_1(t) \quad (2e)$$

$$\frac{d\lambda_2(t)}{dt} = k_i[I(t)][M(t)] - \frac{f_I(t) + f_M(t)}{V}\lambda_2(t) - k_{t_1}[K(t)]\lambda_2(t) + [\lambda_0(t) + 2\lambda_1(t)]k_p[M(t)] \quad (2f)$$

$$\frac{d\omega_0(t)}{dt} = k_{t_1}[K(t)]\lambda_0(t) - \frac{f_I(t) + f_M(t)}{V}\omega_0(t) \quad (2g)$$

$$\frac{d\omega_1(t)}{dt} = k_{t_1}[K(t)]\lambda_1(t) - \frac{f_I(t) + f_M(t)}{V}\omega_1(t) \quad (2h)$$

$$\frac{d\omega_2(t)}{dt} = k_{t_1}[K(t)]\lambda_2(t) - \frac{f_I(t) + f_M(t)}{V}\omega_2(t) \quad (2i)$$

where [ ] indicates molar concentration, V is the constant reactor volume, f_I and f_M are the flows of the initiator solution and the monomer solution, respectively, the superscript f indicates feed stock condition, $\lambda_i = \sum j^i[N_j]$ $(i = 0, 1, 2)$ are the first three moments of the number chain length distribution $[N_j]$ vs. j, and $\omega_i = \sum j^i[P_j]$ $(i = 0, 1, 2)$ are the first three moments of the number chain length distribution $[P_j]$ vs. j.

Several variables may be derived from the model of eqs. (2). For example, the instantaneous number average chain length and polydispersity of the total polymer in the reactor may be found through

$$\mu_n(t) = \frac{\lambda_1(t) + \omega_1(t)}{\lambda_0(t) + \omega_0(t)} \quad (3)$$

$$D_n(t) = \frac{[\lambda_0(t) + \omega_0(t)][\lambda_2(t) + \omega_2(t)]}{[\lambda_1(t) + \omega_1(t)]^2} \quad (4)$$

The same variables for the "living" polymer fraction are

$$\mu_{n,l}(t) = \frac{\lambda_1(t)}{\lambda_0(t)} \quad (5)$$

$$D_{n,l}(t) = \frac{\lambda_0(t)\lambda_2(t)}{\lambda_1^2(t)} \quad (6)$$

and analogous expressions for $\mu_{n,d}(t)$ and $D_{n,d}(t)$ may be written, in relation to the deactivated polymer fraction. Two definitions for the instantaneous polymer production (in mass per unit time) are possible. One considers only the polymer leaving the reactor, which may be calculated from:

$$\tilde{z}(t) = M_m[f_I(t) + f_M(t)][\lambda_1(t) + \omega_1(t)] \quad (7)$$

where M_m is the monomer molecular weight. The other also considers the instantaneously accumulated polymer inside the reactor as follows:

$$z_i(t) = VM_m \frac{d[\lambda_1(t) + \omega_1(t)]}{dt} + \tilde{z}(t) \quad (8)$$

Equations (2e), (2h), (7) and (8) finally yield

$$z_i(t) = VM_m\{k_i[M(t)][I(t)] + k_p[M(t)]\lambda_0(t)\} \quad (9)$$

When the feed flows are periodic functions [i.e., $f_I(t) = f_I(t + T_p)$ and $f_M(t) = f_M(t + T_p)$, where T_p is a fixed period of oscillation], then all reactor variables such as $[I(t)]$, $[K(t)]$, $\lambda_i(t)$, $\omega_i(t)$, $\mu_n(t)$, and $z_i(t)$ will all eventually become periodic, and of the same period. The quality of a polymer ob-

tained under periodic operation is represented by the average properties of the accumulated effluent along an integer number of periods of oscillation. We shall indicate these properties by the superscript *. The average moments of the "living" and deactivated polymer fractions may be calculated through similar expressions. For example, in the latter case,

$$\omega_i^* = \frac{\int_t^{t+T_p} [f_I(\tau) + f_M(\tau)]\omega_i(\tau)\, d\tau}{\int_t^{t+T_p} [f_I(\tau) + f_M(\tau)]\, d\tau}, \quad (i = 0, 1, 2) \tag{10}$$

Then, the average values of the number-average chain length and the polydispersity are obtained from

$$\mu_n^* = \frac{\lambda_1^* + \omega_1^*}{\lambda_0^* + \omega_0^*} \tag{11}$$

$$D_n^* = \frac{(\lambda_0^* + \omega_0^*)(\lambda_2^* + \omega_2^*)}{(\lambda_1^* + \omega_1^*)^2} \tag{12}$$

The average polymer production per unit time under periodic operation z may be calculated from

$$z = \frac{M_m}{T_p} \int_t^{t+T_p} [f_I(\tau) + f_M(\tau)][\lambda_1(\tau) + \omega_1(\tau)]\, d\tau \tag{13}$$

Similarly, the average conversions η_I^* and η_M^* of initiator and monomer are respectively given by

$$\eta_I^* = \frac{\int_t^{t+T_p} [f_I(\tau) + f_M(\tau)][\lambda_0(\tau) + \omega_0(\tau)]\, d\tau}{[I^f] \int_t^{t+T_p} f_I(\tau)\, d\tau} \tag{14}$$

$$\eta_M^* = 1 - \frac{\int_t^{t+T_p} [f_I(\tau) + f_M(\tau)][M(\tau)]\, d\tau}{[M^f] \int_t^{t+T_p} f_M(\tau)\, d\tau} \tag{15}$$

Note that, in eq. (14), only the conversion of initiator into polymer has been considered.

The Optimal Periodic Control Problem

The scalar functional to be minimized is written as the sum of three terms, each consisting of deviations from the desired values of μ_n^*, D_n^*, and z (represented by superscript d), as follows:

$$J = \frac{w_1}{[D_n^d]^2}[D_n^* - D_n^d]^2 + \frac{w_2}{[\mu_n^d]^2}[\mu_n^* - \mu_n^d]^2 + \frac{w_3}{[z^d]^2}[z - z^d]^2 \tag{16}$$

where w_1, w_2, and w_3 are adjustable weights.

The aim is to find two periodic functions $f_I(t)$ and $f_M(t)$ such that $J \cong 0$. To this effect, the approach developed in Frontini et al.[2] can be applied to the expanded system of eqs. (2); and the resulting equations are presented in the Appendix. For a fixed period of oscillation, the periodic control policy is iteratively calculated, starting from low-amplitude sinusoidal perturbations, around a chosen optimal SS condition.

Indicating any possible SS by the superscript s, the optimal SS is that which minimizes the functional of eq. (16); but with D_n^*, μ_n^* and z replaced by D_n^s, μ_n^s, and z^s, respectively. Since $D_n^s \cong 2$ for any possible SS, an optimal SS is such that $\mu_n^s = \mu_n^d$ and $z^s = z^d$. This condition may be found by appropriate selection of the design and operational inputs V, f_M, f_I, $[M^f]$, $[I^f]$, and $[K^f]$.

The period of oscillation exerts a profound influence on D_n^*.[3] Thus, T_p must be adequately selected, prior to minimizing J. This parameter and the phase shift T between the sinusoidal feed flows proposed as initial perturbations for the iterative algorithm may be simultaneously determined through the sensitivity analysis technique suggested in Frontini et al.[2]

The direct extremizations (i.e. maximization and minimization) of D_n^* help in determining an "unrestricted" range for the average polydispersity. In general, the feasible range for D_n^* in the "restricted" J functional constitutes a subset of the first. A lower polydispersity than the limit determined by min D_n^* may be possibly found if the polymerization is carried out in a batch reactor. Ideally, Poisson MWD's with $D_n \cong 1$ are obtained in the case of nonterminated batch polymerizations with instantaneous initiation. Under the presence of impurities, the low molecular weight tail of the dead polymer that builds up along a batch polymerization, considerably broadens the final MWD.[4] With slow initiation with respect to propagation, the resulting Gold MWD is also wider than the Poisson MWD. It may be useful to compare the average polydispersity obtained through min D_n^*, with the polydis-

persity observed at the end of an equivalent batch polymerization.

Except for D_n^d, the other two specifications are already reachable in the SS. For this reason, the problem of min J with $D_n^d < 2$ is essentially equivalent to that of min D_n^*; and the problem of min J with $D_n^d > 2$ is equivalent to that of max D_n^*. Furthermore, identical or nearly identical combinations of parameters T and T_p are to be expected for these two classes of problems.[2]

The optimization procedure may be summarized as follows:

1. From a global SS analysis, select an optimal SS that provides acceptable values for $\mu_n^d = \mu_n^s$ and $z^d = z^s$.
2. Through the sensitivity analysis, determine the best combinations for the period of oscillation T_p and the phase of the initial sinusoidal perturbations T, in order to start the iterative procedures of max D_n^* and min D_n^*, from the optimal SS.
3. Extremize D_n^*, and select some feasible D_n^d. (In general, values of D_n^d either above or below the SS value of 2 will be possible.) For all optimal periodic control calculations, the amplitudes of the initial perturbations were adopted 0.02 of their optimal SS values.
4. Having specified J, apply the sensitivity analysis again, to find T and T_p for this functional.
5. Minimize J as follows: (a) Apply the initial sinusoidal perturbations to the system model of eqs. (2); (b) solve the costate eqns (A.14)–(A.22); (c) improve the controls through eqs. (A.9)–(A.10) and (A.23)–(A.24); (d) solve the state equations (2); and repeat steps (b)–(d) until no significant improvement in J is observed.

Polydispersity Maximization by Blending of Two Schulz–Flory Distributions

As we shall see below, impurities introduce upper and lower bounds in the range of obtainable molecular weights, thus inhibiting the production of high polydispersity polymers. If the CSTR is operated for long time intervals at a bound, then a Schulz–Flory MWD will be produced during such intervals.

In this section, the increase in polydispersity by mixture of two Schulz–Flory distributions will be investigated. Assume two polymer components with the following weight chain length distributions:

$$\text{Polymer 1: } q_1(j) = \frac{j}{\mu_{n_1}^2}\exp\left(-\frac{j}{\mu_{n_1}}\right) \qquad (j = 1, 2, 3, \cdots) \quad (17)$$

$$\text{Polymer 2: } q_2(j) = \frac{j}{\mu_{n_2}^2}\exp\left(-\frac{j}{\mu_{n_2}}\right) \qquad (j = 1, 2, 3, \cdots) \quad (18)$$

Calling y the weight fraction of Polymer 1, the weight chain length distribution of the total polymer results:

$$q(j) = yq_1(j) + (1 - y)q_2(j) \qquad (j = 1, 2, 3, \cdots) \quad (19)$$

Replacing eqs. (17) and (18) in eq. (19), and this in turn into $\mu_n = \sum [q(j)/j]^{-1}$, the number average chain length of the final polymer yields

$$\mu_n(y) = \frac{\mu_{n_1}\mu_{n_2}}{y\mu_{n_2} + (1 - y)\mu_{n_1}} \quad (20)$$

Similarly, from eqs. (17)–(19) and $\mu_w = \sum [jq(j)]$, one may obtain

$$\mu_w(y) = 2[y\mu_{n_1} + (1 - y)\mu_{n_2}] \quad (21)$$

From eqs. (20) and (21), the following expression for D_n may be derived:

$$D_n(y) = 2\left(\frac{\mu_{n_1}}{\mu_{n_2}} + \frac{\mu_{n_2}}{\mu_{n_1}} - 2\right) \times \left(y - y^2 + \frac{1}{\dfrac{\mu_{n_1}}{\mu_{n_2}} + \dfrac{\mu_{n_2}}{\mu_{n_1}} - 2}\right) \quad (22)$$

For fixed values of μ_{n_1} and μ_{n_2}, $D_n(y)$ represents a parabola that crosses through points (0, 2) and (1, 2), and exhibits a maximum at $y = 0.5$. Furthermore, this maximum may be obtained from

$$D_{n,\max} = 2 + \frac{1}{2}\left(\frac{\mu_{n_1}}{\mu_{n_2}} + \frac{\mu_{n_2}}{\mu_{n_1}} - 2\right) \quad (23)$$

and the corresponding average molecular weight through

$$\mu_{n,\max} = 2\,\frac{\mu_{n_1}\mu_{n_2}}{\mu_{n_1} + \mu_{n_2}} \quad (24)$$

The above result is in accord to Ref. 5, where it was proven that D_n is maximized when equal weights

of two monodisperse polymers, selected at the limits of any given fixed molecular weight range, are blended together.

THE SIMULATED EXAMPLE

Consider, as in Refs. 1, 2, and 6, the polymerization of isoprene in *n*-heptane with *n*-butyllithium as initiator at 25°C, together with the following data: $V = 0.9\ dm^3$; $k_i = 21.47\ dm^3/g\ mol\ h$; $k_p = 4284\ dm^3/g\ mol\ h$; $k_{t_1} = k_{t_2} = 40{,}000\ dm^3/g\ mol\ h$; $[K^f] = 0.005\ g\ mol/dm^3$; and $[M^f] = 6\ g\ mol/dm^3$. Note that although k_i and k_p have been taken from the literature, the termination constants were arbitrarily assigned. Also, $[K^f]$ is about 1 order of magnitude lower than the experimental value assumed in Alassia et al.[4]

Steady-State Analysis

For the given system and the following constant feed rates, $f_I^s = f_M^s = 0.5\ dm^3/h$, Figure 1 illustrates a set of possible SS conditions. The output variables are represented vs. a range of stock initiator concentrations $[I^f]$, and for three different impurities concentrations in the monomer feed $[K^f]$. All curves start at a small positive value of $[I^f]$, because no polymer is obtained with $[I^f] = 0$. The variable $l^s = \lambda_0^s/(\lambda_0^s + \omega_0^s)$ represents the "living" molar fraction of the total polymer. The following general comments can be made:

1. As expected, $D_n^s \cong 2$ for any inputs combination.
2. For $[K^f] = 0$, then z^s, η_I^s, η_M^s, and l^s are higher than when impurities are present; and μ_n^s is unbounded and monotonically decreasing.
3. For $[K^f] > 0$, then: (a) μ_n^s is upper-bounded (with reduced maxima as $[K^f]$ is increased), and lower-bounded (at the low limit of the initiator concentration); and (b) for high initiator concentrations, all "controlled" variables (μ_n^s, D_n^s, and z^s), converge to the impurities-free case.

Consider Figure 1(a), at the chosen concentration $[K^f] = 0.005\ mol/dm^3$. At the maximum, $\mu_n^s \cong 825$ and $f_I^s[I^f] \cong f_M^s[K^f]$, because $k_{t_1} \gg k_i$ and the added initiator moles are enough to "scavenge" practically all impurities. At very low initiator concentrations, μ_n^s cannot be reduced below $\cong 130$. Note that if one aimed at maximizing D_n by mixture of two SS polymers in the range $0 < [I^f] < [I^f]_{max}$, then equal weights of $\mu_{n_1} = 130$ and $\mu_{n_2} = 825$ would be required; and according to eq. (23), $D_{n,max} = 4.25$. This relatively low polydispersity is an indication of the inflexibility introduced by the impurities.

In summary, the following may be stated:

1. In the SS, and presumably under periodic operation too, the impurities severely restrict the feasible ranges of μ_n^d and D_n^d.
2. In the interval $0 < [I^f] < [I^f]_{max}$, the SS polymer production and monomer conversion are intolerably low. In the range $[I^f]_{max} < [I^f] < \infty$, z^s, and η_M^s are acceptable, but the initiator conversion η_I^s is low. (Note, incidentally that functional J does not penalize low values of η_I^* or η_M^*).
3. The SS analysis assumed constant feed flows, but variable initiator stock concentrations $[I^f]$. During the periodic operation, $[I^f]$ is held constant while f_I and f_M are varied. In both cases, however, similar changes in the reagent concentrations [K], [I], and [M] are induced.

Table I indicates the two SSs that were finally selected as starting points for the optimization studies. Such values are also indicated in Figure 1. Steady-state B is technologically more interesting, because it involves larger values of μ_n^s, z^s, η_I^s, and η_M^s. Steady-state A was included to investigate the more abnormal situation, where increases in $[I^f]$ generate also increases in μ_n^s.

The Batch Polymerization Limit

The model of eqs. (2) may be utilized to simulate a batch polymerization as follows: adopting $f_I(t) = f_M(t) = 0$, assuming a set of initial conditions [I(0)], [M(0)], and [K(0)] for the reagent concentrations and taking $\lambda_i(0) = \omega_i(0) = 0$ for $i = 0, 1, 2$.

Batch simulations corresponding to the optimal SSs indicated as A and B in the previous section were implemented. For both SSs, identical flow rates were adopted for f_I and f_M. Therefore, the initial concentrations can be taken as one half of their corresponding stock concentrations, as indicated in the first three rows of Table II.

Call t_f the final batch time required to reach a constant model output. This parameter, together with some of the reactor outputs, are also indicated in Table II. The initiator and the monomer conversions are defined by $\eta_I(t) = \{[I(0)] - [I(t)]\}/[I(0)]$ and $\eta_M(t) = \{[M(0)] - [M(t)]\}/[M(0)]$,

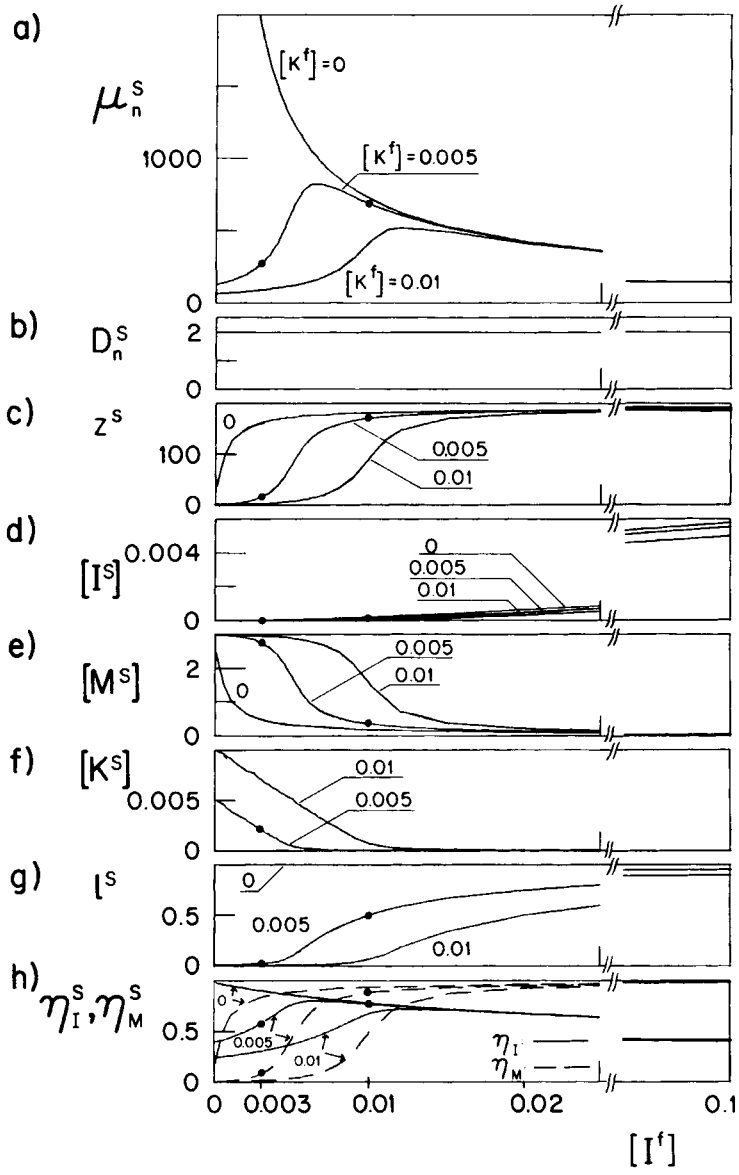

Figure 1 SS outputs for different combination of $[I^f]$ and $[K^f]$.

respectively. Note that the final polydispersity for Batch "A" is above the SS value of 2. This is an indication of potential difficulties if narrow polymers associated with SS "A" were required.

Extremizations of the Average Polydispersity

Consider the minimization and maximization of D_n^* about the previously defined optimal steady states A and B, to obtain feasible ranges for D_n^d. Figures 2(a) and (b) illustrate the sensitivity analysis required to select appropriate T_p and T parameters for such calculations. The variations of D_n^* due to small sinusoidal perturbations of f_I and f_M are represented vs. the frequency of oscillation ($= 2\pi/T_p$), with the phase shift T as parameter. The "best" (T_p, T) combinations are those which produce the highest positive and negative variations in ΔD_n^*, and the finally selected values are presented in the first two rows of Table III. Then, the extremizations of D_n^* provide the "optimal" results shown in the last five rows of Table III. For both starting points, D_n^* is bounded between around 1.5 and 7.5, whereas μ_n^* and z vary with respect to their original SS values. Note that the final average polydispersity for min D_n^* from SS "A" is below the corresponding batch polydispersity of Table II; and the opposite is verified for min D_n^* from SS "B."

Table I The Chosen Optimal SSs

	Optimal SS "A"	Optimal SS "B"
$[I^f]$	0.003 mol/dm^3	0.010 mol/dm^3
$[M^f]$	6 mol/dm^3	6 mol/dm^3
$[K^f]$	0.005 mol/dm^3	0.005 mol/dm^3
$[I^s]$	0.000016 mol/dm^3	0.000570 mol/dm^3
$[M^s]$	2.754 mol/dm^3	0.3512 mol/dm^3
$[K^s]$	0.001038 mol/dm^3	0.000027 mol/dm^3
D_n^s	2.00	2.00
μ_n^s	280	680
z^s	15.7 g/h	170 g/h
η_I^s	0.579	0.777
η_M^s	0.083	0.883
l^s	0.026	0.505

Figures 3(a)-(j) illustrate the optimal periodic profiles for the maximization and the minimization of D_n^*, from steady state A. The following is observed:

1. For min D_n^*, the reagent feeds tend to high pulses, out of phase within each other, thus resembling a semibatch polymerization.
2. For max D_n^*, the number average chain length of the instantaneously produced polymer $\mu_{n,l}(t)$ is most of the time fixed at a low bound, but also exhibits a high peak during a short interval. It is easily shown that the low molecular weight polymer corresponds to the left limit of curve $[K^f] = 0.005$ in Figure 1(a). Since the peak of $f_I(t)$ is large enough to scavenge all impurities, the unrestricted $[K^f] = 0$ case is approached while high molecular weight material is being produced.
3. In the max D_n^* solution, the instantaneous production $z_l(t)$ indicates that the polymer mass generated during the interval when the high molecular weight peak of $\mu_{n,l}(t)$ is observed is nearly identical to the polymer mass produced in the remaining fraction of the period. Thus, the optimal $y = 0.5$ solution of eqs. (22)-(24) seems to be extrapolable to the present more complicated situation, which involves a large variety of high MWDs.

Desired Polymers and Functionals

The selection of $D_n^d = 1.5$ and 4.0 for each optimal SS determines the specifications of the first three rows of Table IV. Call $J_{A_{max}}$, $J_{A_{min}}$, $J_{B_{max}}$ and $J_{B_{min}}$ the corresponding functionals. In all cases, the weights w_1, w_2, and w_3 were taken equal to 1. Note that since D_n^d for A_{min} is below the "unrestricted" bound of 1.52, such specification will be *a priori* unreachable.

The sensitivity analysis for each J functional is presented in Figures 2(c)-(f), and the selected parameters are indicated in the fourth and fifth rows of Table IV. As expected, the same combinations for T_p and T were adopted in the cases of max D_n^*, min $J_{A_{max}}$, and min $J_{B_{max}}$, but small differences appear for min D_n^*, min $J_{A_{min}}$, and min $J_{B_{min}}$.

Optimal Periodic Control

Figures 4 and the last three rows of Table IV summarize the optimal periodic control results. Note the following:

1. Although the specifications of polymers A_{max} and B_{min} are accurately met, deviations appear for polymers A_{min} and B_{max}.
2. The final average polydispersity of A_{min} is 1.95 instead of 1.5, in spite of the fact that the periodic forcing resembles a semibatch operation. In this case, the restriction imposed by the production term determines that the instantaneously produced polymer may be defined by a Schulz–Flory MWD of a virtually constant $\mu_n(t)$. This product is similar to that observed at the left bound of Figure 1(a), for $[K^f] = 0.005$.
3. The average polydispersity of B_{max} is 2.85 instead of 4.0, because (unlike the case of max D_n^* for steady-state B) the controls were unable to surpass the upper bound of $\mu_n(t)$, through an excess of initiator. In this case, the term of μ_n constitutes the main restriction.
4. When a polymer with $D_n^d < 2$ is required (i.e., for min D_n^* SSs A or B, min $J_{A_{min}}$, and min

Table II Batch Polymerization Results

	Batch "A"	Batch "B"
[I(0)]	0.0015 g mol/dm^3	0.005 g mol/dm^3
[M(0)]	3.0 g mol/dm^3	3.0 g mol/dm^3
[K(0)]	0.0025 g mol/dm^3	0.0025 g mol/dm^3
t_f	1.0 h	0.75 h
$D_n(t_f)$	2.34	1.34
$\mu_n(t_f)$	221	814
$\eta_I(t_f)$	1	1
$\eta_M(t_f)$	0.051	1
$l(t_f)$	0.000	0.77

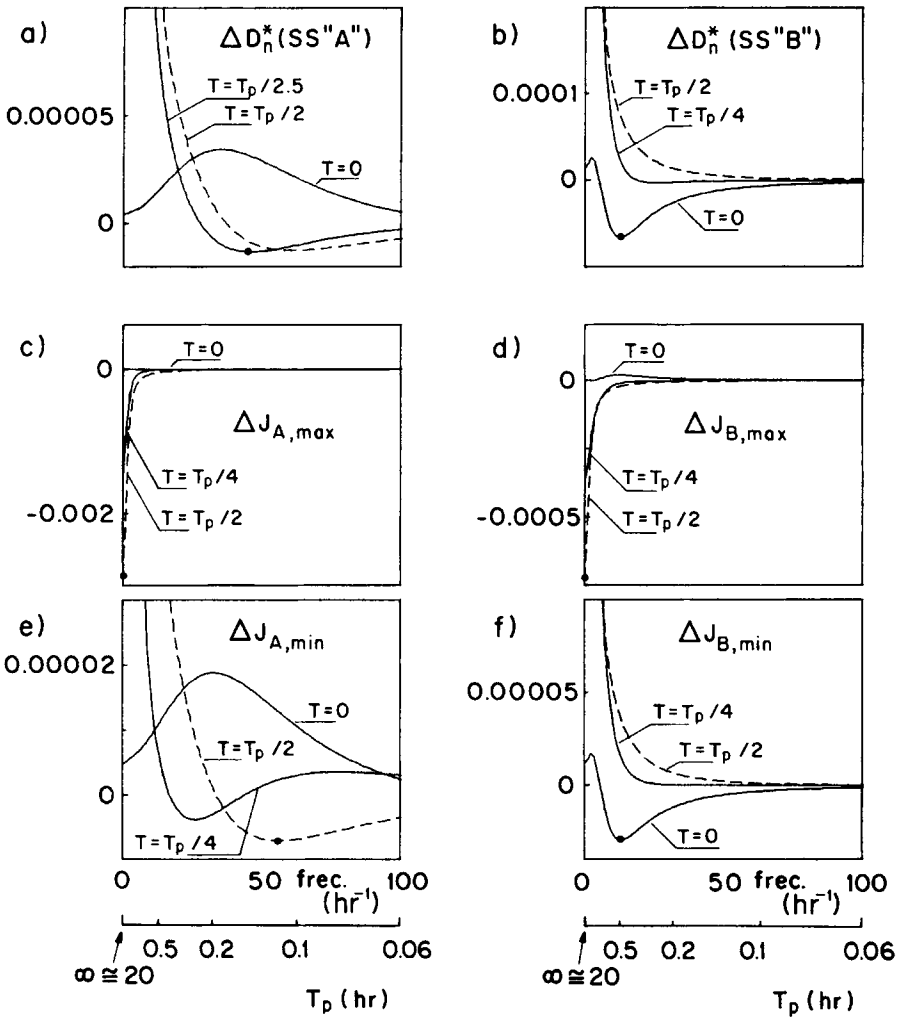

Figure 2 Sensitivity analysis for the selection of T_p and the phase T of the initial sinusoidal perturbations: (a, b) variations of D_n^*; (c–f) variations of the four final functionals.

$J_{B_{min}}$), the average production under periodicity conditions (z) results in a value higher than the original optimal SS value (z^s). It seems unreasonable to force the system to reduce average production; therefore, the production term should not have been included in the above-mentioned J functionals.

DISCUSSION

Even small amounts of impurities have a profound influence on the polymer obtained through "living" anionic polymerizations carried out in periodically forced CSTRs.[1] Therefore, such impurities have to be taken into consideration for a realistic optimal periodic control calculation. This implied the numerical solution of 18 differential equations (be-

Table III Extremizations of D_n^*

	From Optimal SS "A"		From Optimal SS "B"	
	max D_n^*	min D_n^*	max D_n^*	min D_n^*
T_p (h)	20	0.14	20	0.5
T	$T_p/2$	$T_p/2.5$	$T_p/2$	0
D_n^*	7.71	1.52	7.37	1.44
μ_n^*	302	342	303	700
z (g/h)	10.0	182	36.2	176
η_I^*	0.50	0.50	0.35	0.84
η_M^*	0.05	0.12	0.33	0.55

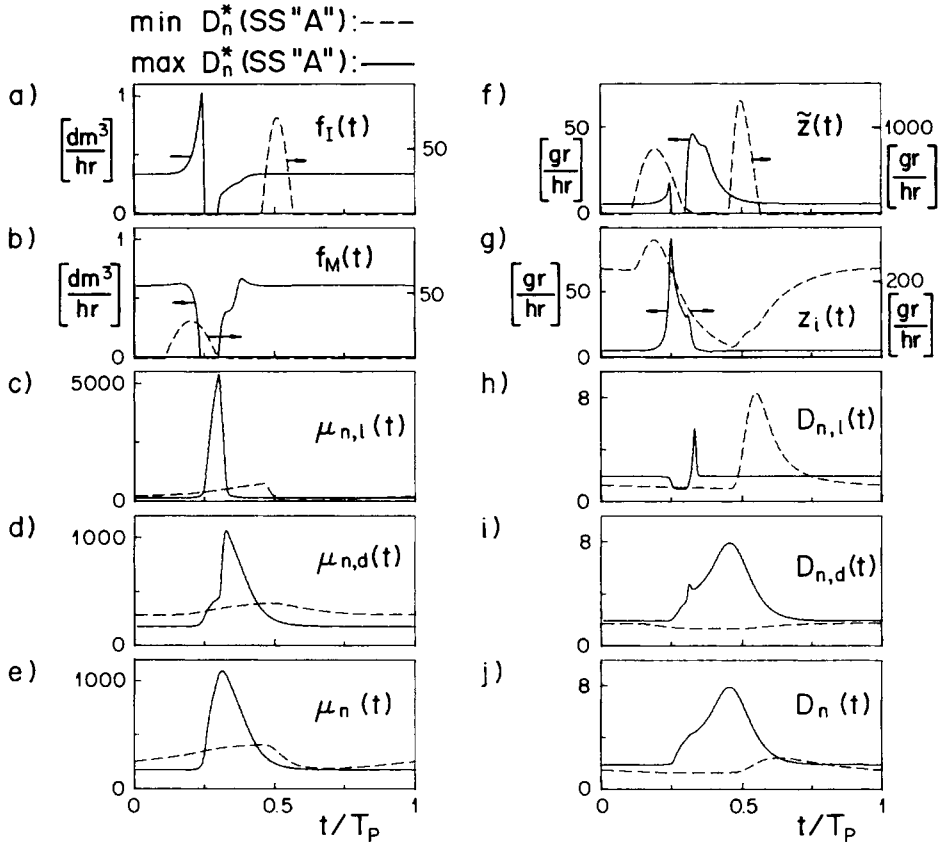

Figure 3 Optimal profiles for the maximization and minimization of D_n^* around the optimal SS "A".

tween states and costates), instead of 10 for the impurities-free model of Refs. 2 and 6. However, the same theoretical approach developed for the simpler case of Ref. 2 could be directly applied to the present more comprehensive model.

Impurities severely affect the advantages of periodic operation, especially when broad MWDs are required. For the simulated isoprene polymerization, the range between min D_n^* and max D_n^* is narrowed from 1.13/12.7 for the impurities-free case,[2] to about 1.5/7, when $[K^f] = 0.005$ mol/dm^3. This is due to the appearance of bounds in the average molecular weights of the produced polymer. Also, when the initiator feed is below a critical value (where practically all impurities are "scavenged"), and inverse behavior from the control point of view is observed, in the sense that increases in the monomer to initiator concentration reduce the average molecular weight. The global SS analysis proved valuable for selecting appropriate optimal SS conditions, and also for detecting potential difficulties associated with bounds or abnormal behaviors.

Table IV Products Specifications, Required T, T_p Parameters, and Optimal Periodic Control Results

	Polymer A_{max}	Polymer A_{min}	Polymer B_{max}	Polymer B_{min}
D_n^d	4.0	1.5	4.0	1.5
μ_n^d	280	280	680	680
z^d (g/h)	15	15	170	170
T_p (h)	20	0.11	20	0.5
T	Tp/2	Tp/2	Tp/2	0
D_n^*	4.0	1.95	2.85	1.5
μ_n^*	285	230	530	680
z (g/h)	15.0	17.0	150	175

The maximization of D_n^* involves large periods of oscillation, and the alternating generation of high and low molecular weight material. To adequately interpret some observed periodic solutions, the maximization of average polydispersity via blending of two Schulz–Flory distributions has been investigated. In general, polydispersity is maximized when equal weights of high and low molecular weight material are added together.

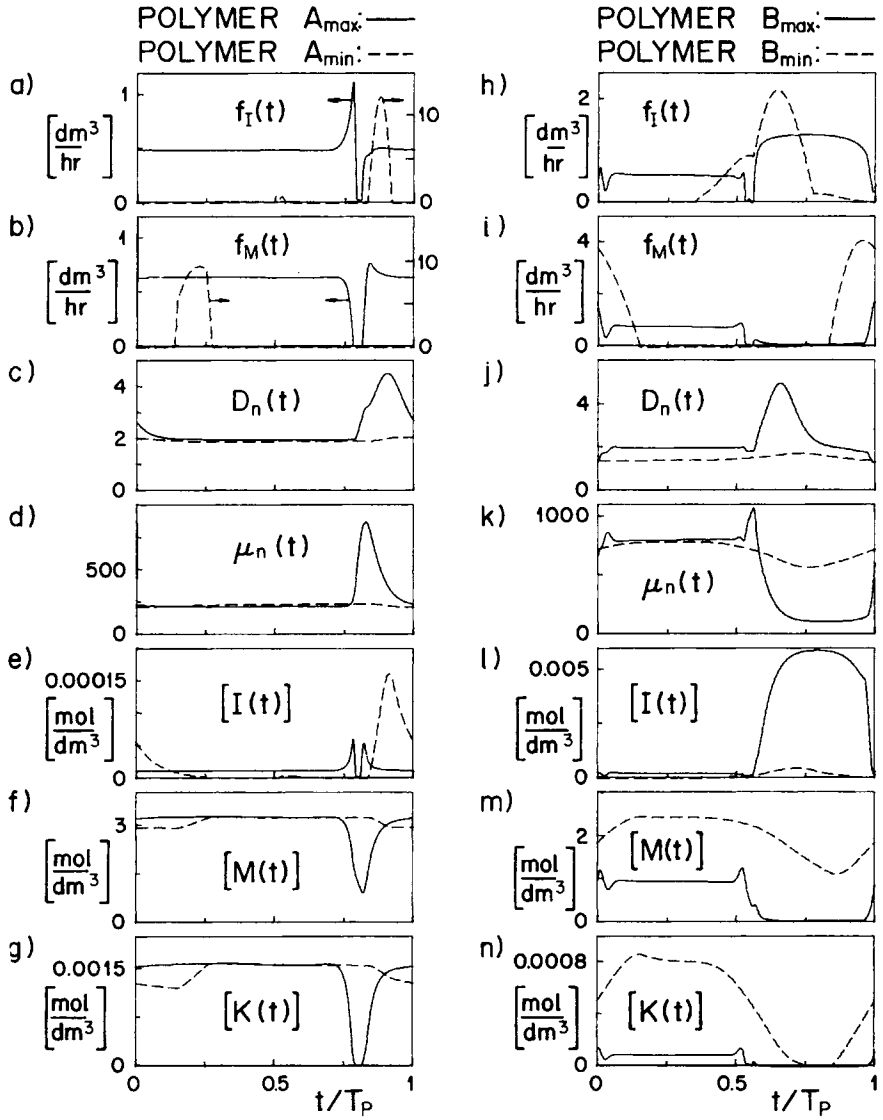

Figure 4 Optimal profiles for the minimization of $J_{A_{min}}$, $J_{A_{max}}$, $J_{B_{min}}$, and $J_{B_{max}}$.

With periods in the order of the average residence time, the periodic operation allows the production of polymers with polydispersities below that of the SS; and the forcing can resemble a semibatch operation. Also, when impurities are present, a batch polymerization does not necessarily produce the narrowest possible MWD. In general, impurities are not a great obstacle for synthesizing polymers with $D_n^* < 2$ because a polymer with an approximately constant average molecule weight (and of a value close to the *a priori* reachable optimal SS) is required in this case.

The production term in eq. (16) is unreasonable if its corresponding SS value is below the average periodic production. Also, the initiator consumption is not even indirectly restricted in eq. (16), and this may lead to technologically unrealistic situations. Both inconvenients could be simultaneously attacked by replacing the production term for $\{w_3[\eta_I^* - 1]^2 + w_4[\eta_M^* - 1]^2\}$, where w_3 and w_4 are weights, and η_I^* and η_M^* are defined by eqs. (14) and (15). This would indirectly impose a cost term on the controls $f_I(t)$ and $f_M(t)$, but the ideal solution would no longer imply that $J \cong 0$.

The investigated isoprene polymerization involved slow initiation with respect to propagation and slow propagation with respect to termination. For this reason, the polymers produce in batch polymerizations were much wider than Poisson distributions (making min D_n^* difficult); and very high

molecular weight material was impossible to obtain (making max D_n^* difficult). For comparison, the styrene polymerization in a benzene/THF mixture at 25°C with *n*-butyllithium and the following data[7] was also investigated: $V = 0.9$ dm^3; $k_i = 1{,}260{,}000$ dm^3/g mol h; $k_p = 126{,}000$ dm^3/g mol h; $k_{t_1} = k_{t_2} = 40{,}000$ dm^3/g mol h; $[M^f] = 0.6$ mol/dm^3; $[I^f] = 0.003$ mol/dm^3; $[K^f] = 0.0005$ mol/dm^3; and $f_I^s = f_M^s = 0.5$ dm^3/h. In this case, the SS analysis indicates that the functions μ_n^s vs. $[I^f]$ are monotonically decreasing and similar to the "unrestricted" $[K^f] = 0$ isoprene case, but starting from finite maxima at the limit of $[I^f] \to 0$. The extremizations of D_n^* indicate a greater flexibility, with the average polidispersity ranging from 1.06 to 43. The optimal periodic control also proved simpler and qualitatively equivalent to the isoprene polymerization with $[K^f] = 0$. This is because impurities are rapidly "scavenged" by the initiator or the "living" polymer.

Finally, the importance of accurate estimations of the intervening parameters should be emphasized. For example, the termination constants are difficult to estimate, but their relative values with respect to k_i and k_p may dramatically alter the optimal profiles. Also, the feed stock concentrations $[K^f]$ and $[I^f]$ are normally difficult to measure; and to his effect, precalibration runs may be necessary.[5] The relatively high parametric sensitivity of the optimal solution with respect to the input coefficients may severely restrict the experimental applicability of the proposed method, but this problem is common to most quantitative anionic polymerization techniques.

REFERENCES

1. L. M. Alassia, G. L. Frontini, J. R. Vega, and G. R. Meira, *J. Polym. Sci. Polym. Lett. Ed.*, **26,** 201 (1988).
2. G. L. Frontini, G. E. Eliçabe, and G. R. Meira, *J. Appl. Polym. Sci.*, **33,** 2165 (1987).
3. D. A. Couso and G. R. Meira, *Polym. Eng. Sci.*, **24**(6), 391 (1984).
4. L. M. Alassia, D. A. Couso, and G. R. Meira, *J. Appl. Polym. Sci.*, **36,** 481 (1988).
5. C. W. Pyun, *J. Polym. Sci. Polym. Ph. Ed.*, **17,** 2111 (1979).
6. G. L. Frontini, G. E. Eliçabe, and G. R. Meira, *J. Appl. Polym. Sci.*, **31**(4), 1019 (1986).
7. S. Bywater and D. J. Worsfold, *Can. J. Chem.*, **40,** 1564 (1962).

Received August 9, 1990
Accepted September 18, 1990

APPENDIX

Equation (9) may be rewritten as follows:

$$J = \frac{w_1}{(D_n^d)^2}\left(\frac{j_1 j_3}{j_2^2} - D_n^d\right)^2 + \frac{w_2}{(\mu_n^d)^2}\left(\frac{j_2}{j_1} - \mu_n^d\right)^2 + \frac{w_3}{(z^d)^2}(M_m j_2 - z^d)^2 \quad \text{(A.1)}$$

with

$$j_i = \frac{1}{T_p}\int_0^{T_p} (f_I + f_M)(\lambda_{i-1} + \omega_{i-1})\, dt \qquad (i = 1, 2, 3) \quad \text{(A.2)}$$

Equations (A.1) and (A.2) may be represented in a more general fashion by

$$J = g(\mathbf{j}) \quad \text{(A.3)}$$

$$\mathbf{j} = \frac{1}{T_p}\int_0^{T_p} \mathbf{m}[\mathbf{x}(t), \mathbf{f}(t)]\, dt \quad \text{(A.4)}$$

where g is a nonlinear scalar function of vector $\mathbf{j}$, $\mathbf{x}(t)$ is the state vector, $\mathbf{f}(t)$ is the control vector, and $\mathbf{m}$ is a vector of nonlinear functions. In our case, $\mathbf{j} = (j_1, j_2, j_3)^T$, $\mathbf{x}(t) = \{[I(t)], [M(t)], [K(t)], \lambda_0(t), \lambda_1(t), \lambda_2(t), \omega_0(t), \omega_1(t), \omega_2(t)\}^T$, $\mathbf{f}(t) = \{f_I(t), f_M(t)\}^T$, and $m_i = (f_I + f_M)(\lambda_{i-1} + \omega_{i-1})$ with $i = 1, 2, 3$. Also, the model of eqs. (2) and its periodicity condition may be symbolized by

$$\mathbf{x}(t) = \mathbf{a}[\mathbf{x}(t), \mathbf{f}(t)] \text{ with } \mathbf{x}(0) = \mathbf{x}(T_p) \quad \text{(A.5)}$$

The minimization of J as defined by eqs. (A.3) and (A.4), and subject to the restrictions of eqs. (A5), may be solved by first defining a Hamiltonian

$$H = \mathbf{p}^T\mathbf{m} + \boldsymbol{\gamma}^T\mathbf{a} \quad \text{(A.6)}$$

where $\mathbf{p} = (p_1, p_2, p_3)^T$ is a real vector calculated through

$$\mathbf{p} = \frac{\partial g}{\partial \mathbf{j}} \quad \text{(A.7)}$$

and $\boldsymbol{\gamma}(t)$ is the costate vector, obtained through the differential system

$$\frac{d\boldsymbol{\gamma}(t)}{dt} = -\frac{\partial H}{\partial \mathbf{x}} \text{ with } \boldsymbol{\gamma}(0) = \boldsymbol{\gamma}(T_p) \quad \text{(A.8)}$$

The extremization of H (and therefore of J) may be numerically solved through a gradient technique that iteratively calculates the necessary controls via the following procedure:

$$f_I(t)|_{new} = f_I(t)|_{old} - \frac{c}{[(1/T_p)\int_0^{T_p} (\partial H/\partial f_I)^2\, dt]^{1/2}} \frac{\partial H}{\partial f_I} \quad (A.9)$$

$$f_M(t)|_{new} = f_M(t)|_{old} - \frac{c}{[(1/T_p)\int_0^{T_p} (\partial H/\partial f_M)^2\, dt]^{1/2}} \frac{\partial H}{\partial f_M} \quad (A.10)$$

with $c > 0$.

For the problem under study, the multipliers defined by eq. (A.7) result:

$$p_1 = 2\frac{w_1}{(D_n^d)^2}\left(\frac{j_1 j_3}{j_2^2} - D_n^d\right)\frac{j_3}{j_2^2} - 2\frac{w_2}{(\mu_n^d)^2}\left(\frac{j_2}{j_1} - \mu_n^d\right)\frac{j_2}{j_1^2} \quad (A.11)$$

$$p_2 = -4\frac{w_1}{(D_n^d)^2}\left(\frac{j_1 j_3}{j_2^2} - D_n^d\right)\frac{j_1 j_3}{j_2^3} + 2\frac{w_2}{(\mu_n^d)^2}\left(\frac{j_2}{j_1} - \mu_n^d\right)\frac{1}{j_1} + 2\frac{w_3}{(z^d)^2}(M_m j_2 - z^d)M_m \quad (A.12)$$

$$p_3 = \frac{2w_1}{(D_n^d)^2}\left(\frac{j_1 j_3}{j_2^2} - D_n^d\right)\frac{j_1}{j_2^2} \quad (A.13)$$

From the Hamiltonian, the costate equations provide:

$$\frac{d\gamma_1(t)}{dt} = \left(\frac{f_I(t) + f_M(t)}{V} + k_i[M(t)] + k_{t_2}[K(t)]\right)\gamma_1(t) + k_i[M(t)]\gamma_2(t) + k_{t_1}[K(t)]\gamma_3(t) - k_i[M(t)]\gamma_4(t) - k_i[M(t)]\gamma_5(t) - k_i[M(t)]\gamma_6(t) \quad (A.14)$$

$$\frac{d\gamma_2(t)}{dt} = k_i[I(t)]\gamma_1(t) + \left(\frac{f_I(t) + f_M(t)}{V} + k_i[I(t)] + k_p\lambda_0(t)\right)\gamma_2(t) - k_i[I(t)]\gamma_4(t) - \{k_i[I(t)] + k_p\lambda_0(t)\}\gamma_5(t) - \{k_i[I(t)] + k_p\lambda_0(t) + 2k_p\lambda_1(t)\}\gamma_6(t) \quad (A.15)$$

$$\frac{d\gamma_3(t)}{dt} = k_{t_2}[I(t)]\gamma_1(t) + \left(\frac{f_I(t) + f_M(t)}{V} + k_{t_2}[I(t)] + k_{t_1}\lambda_0(t)\right)\gamma_3(t) + k_{t_1}\lambda_0(t)\gamma_4(t) + k_{t_1}\lambda_1(t)\gamma_5(t) + k_{t_1}\lambda_2(t)\gamma_6(t) - k_{t_1}\lambda_0(t)\gamma_7(t) - k_{t_1}\lambda_1(t)\gamma_8(t) - k_{t_1}\lambda_2(t)\gamma_9(t) \quad (A.16)$$

$$\frac{d\gamma_4(t)}{dt} = -p_1[f_I(t) + f_M(t)] + k_p[M(t)]\gamma_2(t) + k_{t_1}[K(t)]\gamma_3(t) + \left(\frac{f_I(t) + f_M(t)}{V} + k_{t_1}[K(t)]\right)\gamma_4(t) - k_p[M(t)]\gamma_5(t) - k_p[M(t)]\gamma_6(t) - k_{t_1}[K(t)]\gamma_7(t) \quad (A.17)$$

$$\frac{d\gamma_5(t)}{dt} = -p_2[f_I(t) + f_M(t)] + \left(\frac{f_I(t) + f_M(t)}{V} + k_{t_1}[K(t)]\right)\gamma_5(t) - 2k_p[M(t)]\gamma_6(t) - k_{t_1}[K(t)]\gamma_8(t) \quad (A.18)$$

$$\frac{d\gamma_6(t)}{dt} = -p_3[f_I(t) + f_M(t)] + \left(\frac{f_I(t) + f_M(t)}{V} + k_{t_1}[K(t)]\right)\gamma_6(t) - k_{t_1}[K(t)]\gamma_9(t) \quad (A.19)$$

$$\frac{d\gamma_7(t)}{dt} = -p_1[f_I(t) + f_M(t)] + \left(\frac{f_I(t) + f_M(t)}{V}\right)\gamma_7(t) \quad (A.20)$$

$$\frac{d\gamma_8(t)}{dt} = -p_2[f_I(t) + f_M(t)] + \left(\frac{f_I(t) + f_M(t)}{V}\right)\gamma_8(t) \quad (A.21)$$

$$\frac{d\gamma_9(t)}{dt} = -p_3[f_I(t) + f_M(t)] + \left(\frac{f_I(t) + f_M(t)}{V}\right)\gamma_9(t) \quad (A.22)$$

Finally, the Hamiltonian gradients of eqs. (A.9) and (A.10) yield

$$\frac{\partial H}{\partial f_I} = p_1(\lambda_0 + \omega_0) + p_2(\lambda_1 + \omega_1) + p_3(\lambda_2 + \omega_2) + \frac{[I^f]\gamma_1}{V} - \frac{[I]\gamma_1}{V} - \frac{[M]\gamma_2}{V} - \frac{[K]\gamma_3}{V} - \frac{\lambda_0\gamma_4}{V} - \frac{\lambda_1\gamma_5}{V} - \frac{\lambda_2\gamma_6}{V} - \frac{\omega_0\gamma_7}{V} - \frac{\omega_1\gamma_8}{V} - \frac{\omega_2\gamma_9}{V} \quad \text{(A.23)}$$

$$\frac{\partial H}{\partial f_M} = p_1(\lambda_0 + \omega_0) + p_2(\lambda_1 + \omega_1) + p_3(\lambda_3 + \omega_3) + \frac{[M^f]\gamma_2 + [K^f]\gamma_3}{V} - \frac{[I]\gamma_1}{V} - \frac{[M]\gamma_2}{V} - \frac{[K]\gamma_3}{V} - \frac{\lambda_0\gamma_4}{V} - \frac{\lambda_1\gamma_5}{V} - \frac{\lambda_2\gamma_6}{V} - \frac{\omega_0\gamma_7}{V} - \frac{\omega_1\gamma_8}{V} - \frac{\omega_2\gamma_9}{V} \quad \text{(A.24)}$$